

2 Efficiency of true-green light emitting diodes: 3 non-uniformity and temperature effects

4 Ilya E. Titkov^{1,3,*}, Sergey Yu. Karpov², Amit Yadav³, Denis Mamedov¹, Vera L. Zerova^{3,4}
5 and Edik Rafailov³

6 ¹ Ostendo Technologies Inc., 6185 Paseo del Norte, Carlsbad, CA 92011, USA; ilya.titkov@ostendo.com

7 ² STR Group – Soft-Impact, Ltd., P.O.Box 83, 27 Engels ave., St.Petersburg, 194156, Russia;

8 sergey.karpov@str-soft.com

9 ³ Optoelectronics and Biomedical Photonics Group, Aston Institute of Photonic Technologies,

10 Aston University, Birmingham, B4 7ET, United Kingdom; a.yadav1@aston.ac.uk

11 ⁴ Nanoscale Physics Research Laboratory, School of Physics and Astronomy, University of Birmingham,

12 Birmingham, B15 2TT, United Kingdom; vzerova@gmail.com

13 * Correspondence: ilya.titkov@ostendo.com; Tel.: +1-760-710-3042

14 Academic Editor: name

15 Received: date; Accepted: date; Published: date

16 **Abstract:** External quantum efficiency of industrial-grade green InGaN light-emitting diodes (LEDs)
17 has been measured in a wide range of operating currents at various temperatures from 13 K to 300
18 K. Unlike blue LEDs, the efficiency as a function of current is found to have a multi-peak character,
19 which could not be fitted by a simple ABC-model. This observation correlated with splitting of LED
20 emission spectra into two peaks at certain currents. The characterization data are interpreted in terms
21 of non-uniformity of the LED active region, which is tentatively attributed to extended defects like
22 V-pits. We suggest a new approach to evaluation of temperature-dependent light extraction and in-
23 ternal quantum efficiencies taking into account the active region non-uniformity. As a result, the
24 temperature dependence of light extraction and internal quantum efficiencies have been evaluated
25 in the temperature range mentioned above and compared with those of blue LEDs.

26 **Keywords:** InGaN green LEDs; active region non-uniformity; temperature-dependent electrolumi-
27 nescence; internal quantum efficiency; light extraction efficiency; extended defects; modeling.
28

29 1. Introduction

30 Semiconductor LEDs invented almost 100 years ago [1] have now become key components in
31 numerous applications: solid-state lighting, traffic lights, brake lights, various indicators, and signs
32 [2,3]. For many cases and, especially, for phosphor-free solid state lighting, high-efficiency green LEDs
33 are of primary importance. Nowadays, a new level of external quantum efficiency (EQE), is achieved
34 from commercial green LEDs: ~34% for directly emitting devices and ~54% for those using internal
35 down-conversion of emitted light, see for example [4] that gives overview of the external efficiency of
36 different LED material systems of Osram OS. This progress is a result of both bandgap and strain
37 engineering of the active multiple-quantum-well (MQW) regions, and optimized carrier transport
38 across the LED structures and using advanced chip designs.

39 Nevertheless, the EQE of green LEDs is still remarkably lower than that of blue LEDs, which is
40 now over 70% at the emission wavelengths of 440-450 nm [4]. This fact is a manifestation of the so-
41 called "green gap" problem, i.e. substantial efficiency reduction of InGaN-based LEDs from blue to-
42 wards green/orange spectral range. Among the mechanisms that may be responsible for the "green
43 gap", the ones that are frequently referred are: degradation of InGaN crystal quality at high indium
44 content; polarization field built in the InGaN quantum wells (QWs) and carrier localization due to

45 composition fluctuations in InGaN (see more detailed discussion given in Sec.4.2). To better under-
46 stand the role of each factor plays in this problem, examination of temperature-dependent efficiency
47 is quite constructive.

48 This paper is a natural continuation of our previous study [5] in which temperature dependence
49 of EQE, internal quantum efficiency (IQE) and light extraction efficiency (LEE) of an industrial-grade
50 blue LED emitting at 440-450 nm has been determined in a wide range of temperatures from 13 to 440
51 K. The study [5] was largely based on approximating the dome-like dependence of EQE on cur-
52 rent/output optical power within a simple ABC recombination model. The subject of the present study
53 is a green LED emitting in the range of 530-550 nm (so-called “true-green”). Recently, this method
54 with minor modification has been extended to single-quantum well (SQW) LEDs operating at longer
55 emission wavelengths [6]. However, EQEs of the green-emitting multiple quantum wells reported in
56 [7,8] for a wide temperature range of 4-300 K did not exhibit a dome-like dependence on current,
57 demonstrating more complex behavior that could not be fitted by a simple ABC-model. So, more elab-
58 orate approach is required for experimental estimation of IQE and LEE from those or similar charac-
59 terization data. Development of such an approach to evaluation of temperature-dependent efficiency
60 of true-green LEDs is one of the goals of our study.

61 Generally, blue LEDs exhibit a nearly evenly symmetrical dome-like EQE dependence on cur-
62 rent/output power with respect to its value corresponding to the EQE maximum. In contrast, the EQE
63 dependence of green LEDs frequently becomes asymmetric with a more extended low-current wing
64 [9]. To explain that behavior, various mechanisms have been invoked: electron leakage into p-side of
65 the LED structure [10]; delocalization of carriers captured by InGaN composition fluctuations [11];
66 imbalance between the electron and hole injection into InGaN QWs caused by non-equilibrium QW
67 population [12] and suppression of non-radiative recombination at threading dislocations via carrier
68 localization by composition fluctuations in InGaN alloys [13]. In addition, contribution of device self-
69 heating at high current was not reliably excluded in many experimental studies. Therefore, under-
70 standing the nature of the particular efficiency behavior of green LEDs is another goal of this study.

71 Our data obtained with commercial true-green LEDs demonstrate non-ordinary variation of the
72 emission wavelength with current and considerable deviation of EQE from a simple ABC-model. The
73 low temperature measurements enable interpretation of the data in terms of the active region non-
74 uniformity. The ABC-model modified for non-uniform QWs allow us to estimate the temperature-
75 dependent LEE.

76 2. Experimental

77 2.1. Samples and characterization techniques

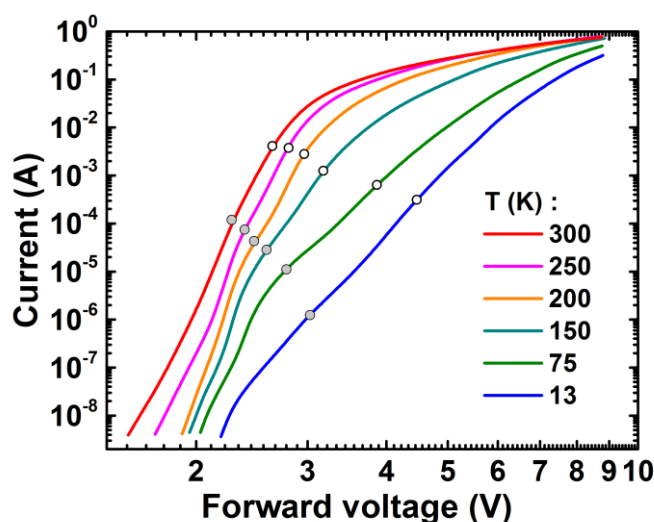
78 The LED samples and characterization techniques utilized herein were quite similar to those used
79 in our previous research [5]. The LED structures were grown by metal-organic chemical vapor depo-
80 sition on C-plane sapphire and consisted (from bottom to top) of an undoped GaN layer followed by
81 a Si-doped n-GaN contact layer, undoped InGaN/GaN MQW active region, a p-AlGaIn electron block-
82 ing layer, and Mg-doped p-GaN contact layer. The main difference from the previously studied blue
83 LEDs was a higher, more than 20%, indium content in InGaN QWs, providing green light emission.
84 The structures were processed as 1×1 mm² UX:3 thin-film chips where high-reflective metallic elec-
85 trodes were formed to the p-contact layer. After removing the sapphire substrate, the back (emitting)
86 surface of the n-contact layer was textured to increase LEE, and the current access to the n-contact
87 layer was provided by the metallic column electrodes passing through the 24 blind vias made in the
88 structure and uniformly distributed over the emitting surface of the die [14]. The total area covered by
89 vias did not exceed 0.5% of the emitting surface area. The chips were mounted onto the Dragon pack-
90 ages without any molding, which is suitable for temperature-dependent electroluminescence meas-
91 urements.

92 A Labsphere spectrometer CDS-600, Keithley 2400 source-meter and Janis CCS-450 helium
93 closed-cycle cryostat were used for temperature- and current-dependent electroluminescence (T-I
94 DEL) technique. In order to determine EQE, we measured electroluminescence (EL) over a wide range

95 of operating current, from 20 nA to 800 mA. To cover the corresponding range of the output optical
 96 power, from 1 nW to 600 mW, we varied spectrometer exposure time from 1 ms to 5 s and used neutral
 97 ND1-4 filters. For calibration of EQE values, EL was measured both in an integrating sphere and in
 98 the cryostat at room temperature (RT). Then optical alignment was not changed at lower temperatures.
 99 The current-voltage (I-V) characteristics were measured with Keithley 4200 semiconductor character-
 100 ization system that provided extended current range.

101 2.2. Current-voltage characteristics

102 Current-voltage characteristics (I-V curves) of the green LED measured at various temperatures
 103 (13-300 K) are shown in Figure 1. As expected, every high temperature curve can be seen in two parts:
 104 the first one below ~3 Volts has a higher slope and can be associated with the carrier injection into the
 105 active region; the second one, above ~3 V, is controlled by the series resistance. No defect-mediated
 106 shoulders can be distinguished in the high-temperature I-V curves in contrast to those observed for
 107 blue LED [5]. However, one can see some traces of such shoulders in the low-temperature curves,
 108 looking like waving at the lower voltages (see also discussion on this issue in Sec.4.3).



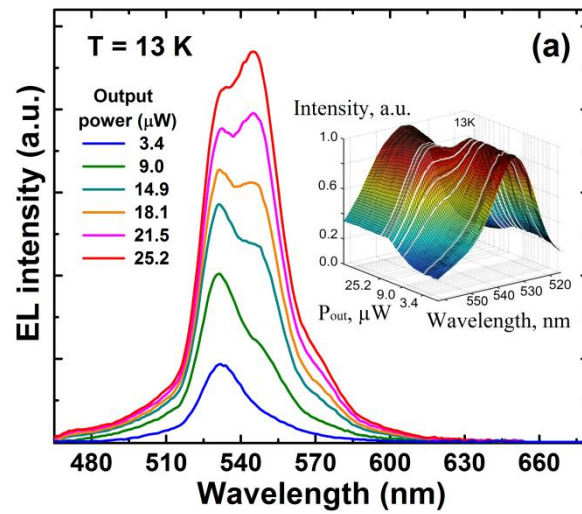
109
 110 **Figure 1.** Current-voltage characteristics of the green LED measured at various temperatures. Closed
 111 and open circles indicate points at which shorter-wavelength and longer-wavelength emission ap-
 112 proaches their maximum efficiency (see Figure 3 and text for more details).

113 Fitting of the I-V curves with Shockley's diode equation accounting for the LED series resistance
 114 has shown that in the temperature range of 200-300 K the curves can be characterized by the ideality
 115 factor of ~3-5 and series resistance of ~7.3-7.6 Ω . For comparison, the ideality factors typical for blue
 116 LEDs [5] were about 1.7 with series resistance ~6.3-6.5 Ω . The relatively high ideality factor may be the
 117 evidence for impeded carrier transport over the barriers between the QWs [15], which correlates with
 118 much deeper InGaN QWs in green LEDs compared to blue ones, or high asymmetry in the donor and
 119 acceptor concentrations in the LED p-n junction [16].

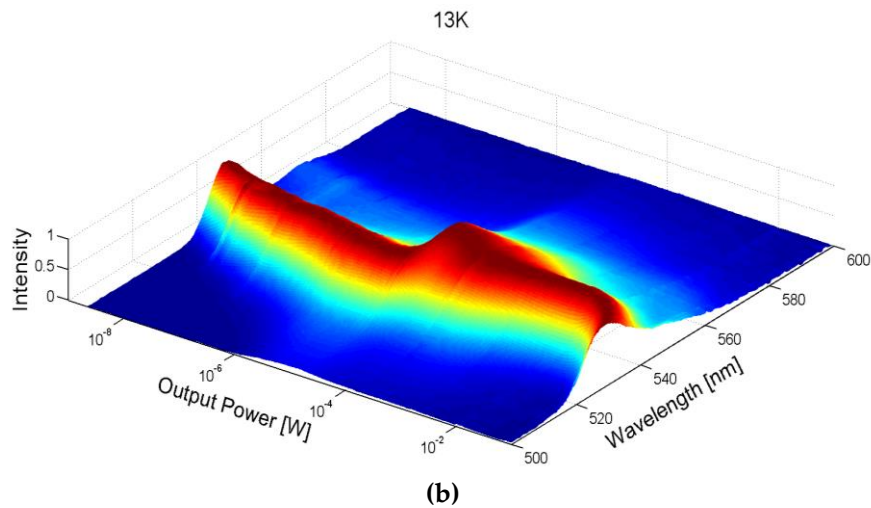
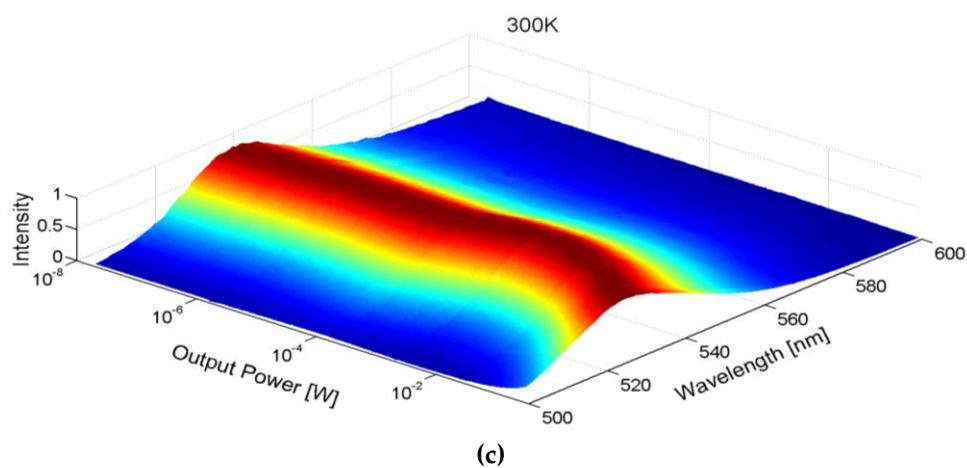
120 At temperatures lower than 200 K, the character of the I-V curves changes dramatically. We be-
 121 lieve that to originate from hole freezing out in the p-layers of LED structure because of a high activa-
 122 tion energy of Mg acceptors. The reduction in the hole density in the p-GaN layer leads to less efficient
 123 thermionic emission or direct tunneling of holes across the metal-GaN interface. Moreover, an addi-
 124 tional electric field in the p-GaN layer is required to maintain the current flow [17]. Identification of
 125 the carrier transport mechanism dominating at low temperatures requires, however, more detailed
 126 investigations that are beyond of this study.

127 2.3. Emission spectra

128 The EL spectra of the green LED were monitored over a wide range of currents and temperatures.
 129 We found the spectra to consist of two main partly merged peaks (see Figure 2a).



130

131
132133
134

135 **Figure 2.** Emission spectra of the green LED at 13 K at various output power (a) where the insert shows
 136 these normalized spectra in 3D vision with additional one at 12 μW ; and evolution of the normalized
 137 emission spectra vs. output power at 13 K (b) and 300 K (c).

138 One of them centered at about 535 nm and referred to hereafter as shorter-wavelength (sw) emission,
 139 was dominant at low output power. Another one centered at ~ 545 nm and referred to hereafter as

140 longer-wavelength (lw) emission, became stronger at higher output power. The peaks competed with
 141 each other in a narrow range of power variation. This two-peak structure of the emission spectra was
 142 clearly seen at temperatures below 200 K and became blurred toward 300 K. A shoulder observed at
 143 $\sim 565\text{-}570$ nm (Figure 2a) was attributed to LO phonon replica, as it was red-shifted with respect to the
 144 lw-peak by the optical phonon energy of $\sim 80\text{-}90$ meV. A similar but much more pronounced LO pho-
 145 non replica was observed previously in the emission spectra of InGaN/GaN quantum wells [5,17]. The
 146 shoulder was observed at temperatures lower than 100 K; at higher temperatures it could be resolved
 147 because of thermal broadening of the phonon replica.

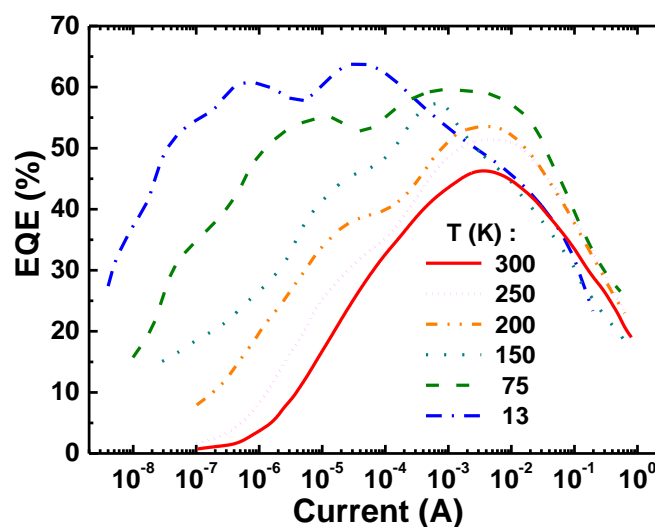
148 In order to understand better the behavior of EL spectra, we examined their normalized intensity
 149 vs. output power. For this purpose, 3D contour plots were generated using the Matlab programming
 150 framework. We processed and stored the measured EL intensity I as a function of wavelength λ and
 151 corresponding emission power P for each temperature. Spectra obtained in such a way were then
 152 normalized to a maximum intensity at every value of P . Then we created continuous normalized func-
 153 tions $I(P, \lambda)$ using linear interpolation of the scattered data. The functions $I(P, \lambda)$ obtained for cryogenic
 154 (13 K) and room (300 K) temperatures are plotted in Figure 2b,c using a log-spaced variable resolution
 155 along the P axis.

156 Figure 2b demonstrates that transition from sw- to lw-emission peaks occurs in a very narrow
 157 range of optical power (transition region) from $\sim 6 \times 10^{-6}$ to $\sim 5 \times 10^{-5}$ W. Beyond this range both peaks
 158 exhibit blue shifts with growing P and overlap partly in the transition region. Similar evolution of the
 159 normalized emission spectra is observed at the temperatures from 13 K to 200 K. At temperatures over
 160 200 K, however, the sw- and lw- peaks are almost indistinguishable in the normalized spectra, Figure
 161 2c. Nevertheless, the transition region is represented via bowing of the EL peak towards longer wave-
 162 lengths at $P \sim 10^{-3}\text{-}10^{-2}$ W.

163 Summarizing the emission spectra behavior, one can see that the transition from the sw- to the
 164 lw-emission peak occurs in a narrow range of output power and has a “switching” character. Outside
 165 the narrow transition region, single sw- or lw-emission peaks dominate at low and high currents, re-
 166 spectively.

167 2.4. Emission efficiency

168 The output power (P) and centroid wavelength measured at various temperatures versus oper-
 169 ating current were converted to EQE and presented in Figure 3. The same EQE data plotted vs. P
 170



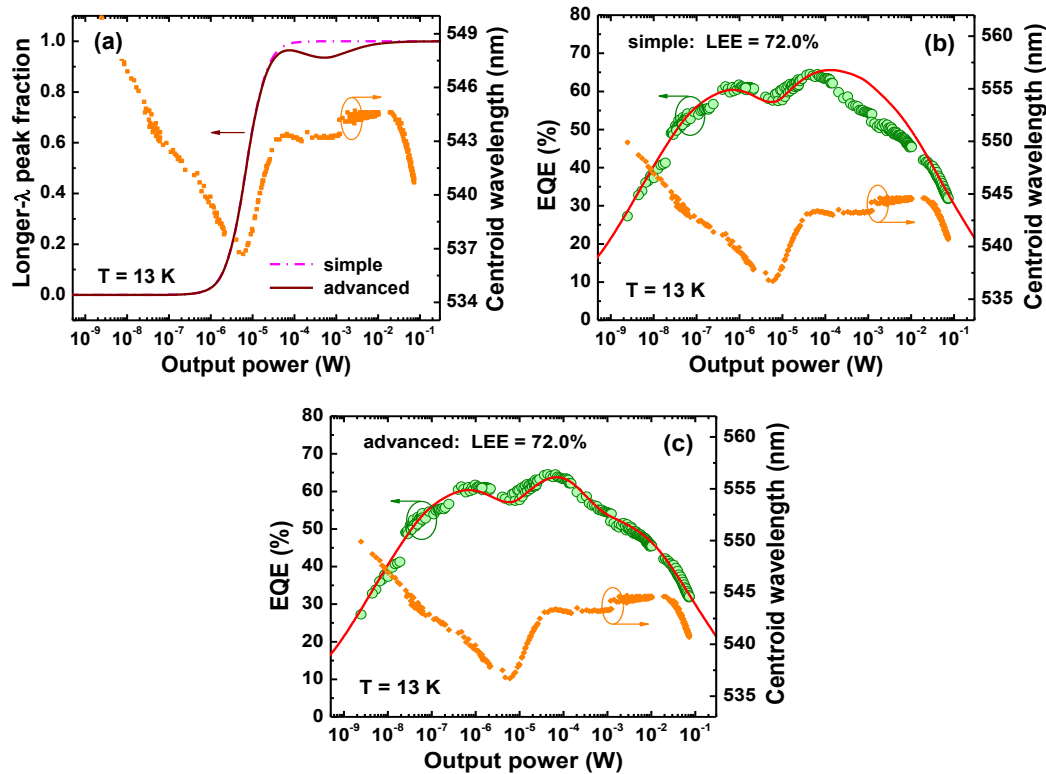
171

172

Figure 3. EQEs of green LED versus driving current measured at various temperatures.

173 are presented separately for every single temperature at Figures 4 and 5. Looking at the low tempera-
 174 ture EQE curves for 13 K and 75 K, one can see a distinct two-peak shape with local maxima located

175 at notable different values of the current/output power. At higher temperatures above 75 K, the low-
 176 current peaks gradually transform to the shoulders and merge with high-current peaks. Unlike these
 177 two main peaks, the third one becomes apparent at low temperatures and low current only, $\sim 0.1 \mu\text{A}$.
 178 This behavior differs from one observed previously with blue LED which was an evenly symmetrical
 179 dome-like function $\text{EQE}(P)$ on a log-scale.



180

181

182 **Figure 4.** Simple and advanced transition functions used in the simulations (a), EQE of the green LED
 183 at $T = 13 \text{ K}$ predicted by modified ABC-model (solid lines) obtained with simple (b) and advanced (c)
 184 transition functions, and emission wavelength as a function of output optical power. Symbols are ex-
 185 perimental data points.

186 It is also important to note that the local minimum of $\text{EQE}(P)$ is placed between two local maxima
 187 at every temperature and correlated well with transient region between two spectral peaks (see Figure
 188 2) as well as with the red shift of centroid wavelength (Figures 4-5). This observation allows us to
 189 attribute the low-current EQE peak to the sw-emission and high-current one to the lw-emission, re-
 190 spectively.

191 Since the measured two-peak EQE dependencies shown in Figures 4 and 5 could not be approx-
 192 imated with a simple ABC-model, a new approach was developed for evaluation of IQE and LEE of
 193 the green LED.

194 3. Modeling

195 3.1. Model

196 In our previous work [5] IQE and LEE of a commercial blue LED were independently evaluated
 197 from measured EQE vs. forward current (I). The curve $\text{EQE}(I)$ was fitted there with ABC-model using
 198 original method based on the analytic expression for EQE as a function of the normalized optical
 199 power. The experimental multi-peak structure of the EQE dependence on current/output power
 200 shown in Figure 4b,c does not allow fitting by a simple ABC-model, which predicts the efficiency

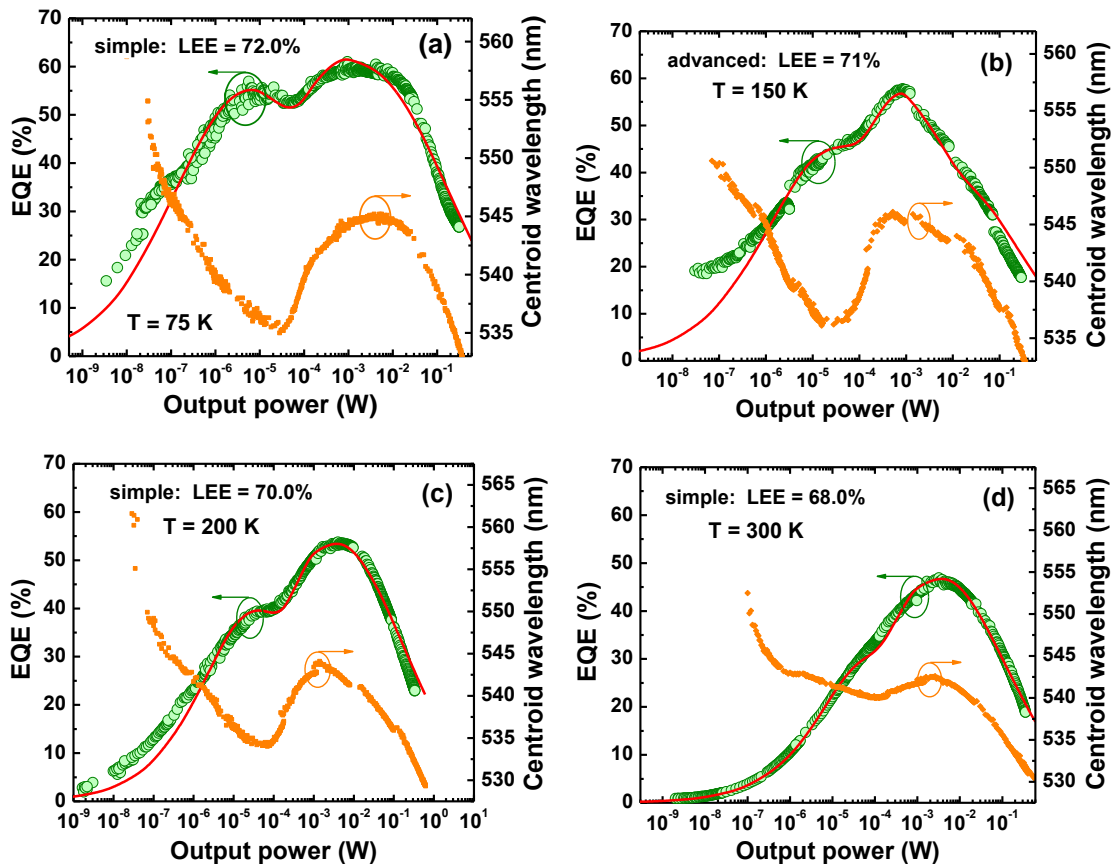


Figure 5. EQE of the green LED and emission wavelength as a function of output power measured at various temperatures (symbols) and predicted by modified ABC-model (solid lines).

to peak at a certain single value of the output power [18]. However, the model can be modified assuming the properties of InGaN QWs in the LED active region (AR) to be non-uniform. The non-uniformity may be attributed to either InGaN composition or the QW width. From the efficiency point of view, various types of non-uniformity are possible. One is the vertical non-uniformity corresponding, for instance, to different InGaN compositions in top and bottom QWs. In this case, the overall IQE of the MQW active region η_i can be regarded in the same manner as used for multi-color LEDs in [19] where

$$\eta_i = \left(\sum_{k=1}^N f_k / \eta_i^{(k)} \right)^{-1}, \quad (1)$$

f_k is the fraction of photons emitted by the k -th QW in the total LED emission spectrum and $\eta_i^{(k)}$ is IQE of the k -th well; summation in (1) is performed over all N QWs.

Another type of non-uniformity is the lateral/in-plane inhomogeneity. Here, different in-plane areas of the AR are assumed to emit light at different wavelengths and to have different IQEs, respectively. Assuming current density to be laterally uniform, one can come again to Eq.(1) connecting η_i with partial efficiencies $\eta_i^{(k)}$ and fractions of emitted photons f_k associated with the above in-plane areas. For brevity, the QWs in the case of vertical non-uniformity and in-plane areas in the case of lateral non-uniformity will be referred to hereafter as different sub-regions (SRs), forming altogether the whole AR of LED structure.

Examination of the LED emission spectra (see Sec. 2.2) has revealed the existence of at least two SRs that emit at different wavelengths. As the LED operating current is increased, the sw-emission is nearly abruptly switched to the lw-emission (see Figure 2b,c). On the other hand, two efficiency peaks can be clearly seen in practically all the EQE plots vs. output optical power P shown in Figure 4b,c and

225 Figure 5. It was already mentioned above, that it is reasonable to attribute the two-peak character of
 226 EQE(P) curves to the existence of two SRs emitting at different wavelengths.

227 As it has been suggested earlier for dual-wavelength LEDs [19], IQE of every particular SR, $\eta_i^{(k)}$,
 228 can be approximated by the analytical expression

$$229 \quad \eta_i^{(k)} = \frac{Q_k}{Q_k + (P_k / P_m^{(k)})^{1/2} + (P_k / P_m^{(k)})^{-1/2}} ; \quad P_k = f_k P, \quad (2)$$

230 where Q_k is the quality factor [18] of the k -th SR, $P_m^{(k)}$ is the optical power corresponding to the IQE
 231 maximum of the k -th SR, and P_k is the optical power produced by the k -th SR at a chosen operating
 232 current. Within the ABC-model, Q_k and $P_m^{(k)}$ are proportional to certain combinations of the recombi-
 233 nation constants: A corresponding to Shockley-Read-Hall non-radiative recombination, B related to
 234 radiative recombination, and C associated with Auger recombination. So, if all f_k are known, the total
 235 IQE of LED structure η_i can be calculated using Eqs.(1)-(2) and then parameters Q_k and $P_m^{(k)}$ can be
 236 fitted to experimental data.

237 Considering just two different SRs to coexist in the whole active region of green LEDs, one can
 238 regard the only fraction f_{lw} corresponding to photons produced by SR with lw-emission; another
 239 fraction attributed to sw-emission is: $f_{sw} = 1 - f_{lw}$. As one can see from Figure 2b, switching between
 240 two spectral peaks occurs in a rather narrow range of the output power. In most of cases the switching
 241 could be well approximated by a simple "transition function"

$$242 \quad f_{lw} = [1 + (P_t / P)^\gamma]^{-1}, \quad (3)$$

243 where P_t is the critical output power corresponding to the transition between the efficiency peaks
 244 (transition power) and the parameter γ is related to the width of the transition region identified on the
 245 log-scale of the output power. We have found $\gamma = 2$ to fit well the transition from shorter to longer
 246 emission wavelength at temperatures from 13 to 250 K. At 300 K, the value $\gamma \sim 1.5$ -1.7 seems to be
 247 more suitable. Nevertheless, we used the parameter $\gamma = 2$ for 300 K as well in order to unify approxi-
 248 mations of the spectral transition at various temperatures.

249 The approximation based on Eq.(3) will be called hereafter as "simple". In some cases, non-mo-
 250 notonous transition functions should be applied to provide more accurate fitting of the characteriza-
 251 tion data. The latter type of the transition function will be referred to as "advanced". In this study, we
 252 used the advanced transition function in the form

$$253 \quad f_{lw} = f_1 \cdot [1 + (P_t / P)^\gamma]^{-1} + \frac{f_2}{1 + (P / P_a) + (P_a / P)}, \quad (4)$$

254 In the particular case presented in Fig.4c, the transition function (4) used the same parameters P_t and
 255 γ as the simple transition function and additional parameters: $f_1 = 0.999998$, $f_2 = 0.2$, and $P_a = 0.5$ mW.
 256 Parameters of the advanced transition function used for calculations shown in Fig.5b differ from the
 257 above ones by only $P_a = 7.0$ mW.

258 3.2. Model application

259 Assuming the light extraction efficiency (LEE) of LED to be the same for the close spectral peaks,
 260 we have fitted EQE(P) curves with Eqs.(1)-(3). For this purpose, parameters Q_k , $P_m^{(k)}$ ($k = sw, lw$), and
 261 P_t were first fitted to provide the best correlation with the multiple-peak dependence of LED efficiency
 262 on the output power. Then IQE was calculated using Eq.(1). Finally, LEE was estimated as a ratio of
 263 experimental EQE and calculated IQE.

264 The dash-dotted line in Figure 4a shows the simple switching function used for fitting of the
 265 EQE(P) measured at $T = 13$ K. The transition power P_t , being the only adjustable parameter of the
 266 transition function, was determined from the observed "switching" in the LED emission spectra from
 267 sw- to lw-emission shown in Fig.2b. The use of the simple switching function with different Q_k and
 268 $P_m^{(k)}$ corresponding to sw ($k = sw$) and lw ($k = lw$) peaks provided the theoretical curve shown by solid
 269 line in Figure 4b at LEE = 72%. The curve fits well the general shape of the EQE(P) dependence but
 270 fails in reproducing some of its details at output power between 10^{-4} and 10^{-2} W. On the other hand,
 271 the spectral evolution of the emission spectra shown in Fig.2b is more complex than it is predicted by
 272 the simple transition function. Therefore, an advanced transition function (solid line in Figure 4a) has
 273 been applied. This enabled much better fitting of the experimental results, as one can see from Figure
 274 4c.

275 Figure 5 presents results of fitting EQE(P) measured at other temperatures. Except for that of 150
 276 K, simple switching functions (4) were sufficient to get a reasonable fitting of the experimental points.
 277 As one can see from the figure, noticeable discrepancy between the fitting and the data is still observed
 278 at low power and $T = 75$ -200 K. This may be the evidence for additional AR non-uniformity, manifest-
 279 ing itself just at extremely low currents. However, we will ignore this possibility in the further discus-
 280 sion, as no evidence for existence of one more distinct spectral peak was found.

281 4. Discussion

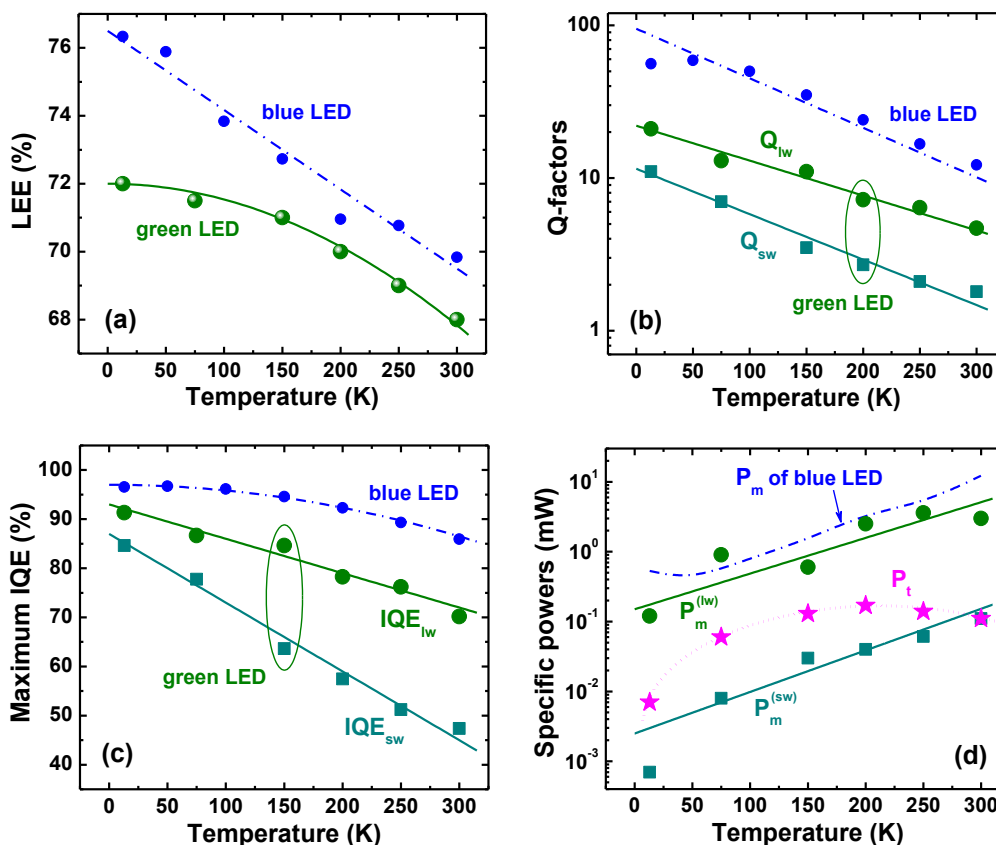
282 This section discusses general trends in variation of important LED characteristics and paramet-
 283 ers with temperature. In order to interpret the trends, we will compare the results obtained for true-
 284 green LED with those reported earlier for blue LED [5].

285 4.1. Light extraction efficiency

286 Figure 6a compares the temperature-dependent efficiencies of light extraction from the LED dice
 287 to air obtained for green and blue LEDs. As one can see from Figure 6, LEE of the green LED is lower
 288 than that of the blue one at all the temperatures. This finding disagrees with the increase in RT LEE
 289 from blue to green spectral range observed on SQW-based LEDs [6]. The LEE increasing with wave-
 290 length was attributed in [6] to temperature dependent optical properties of silver-based p -electrode
 291 providing dominant optical losses of the emitted light via its incomplete reflection from the electrode.
 292 On the other hand, contribution of internal optical losses in the LED die was also found to be consid-
 293 erable. Nevertheless, in LED structures of similar designs, the optical losses have been shown not to
 294 change the general trend of LEE to rise with the emission wavelength [6].

295 The AR of the green LED differs from those studied in [6] in two aspects. First, it consists of five
 296 InGaN QWs, which makes band-to-band light absorption quite critical for achieving high LEE. Sec-
 297 ondly, the AR non-uniformity of the green LEDs results in two different spectral peaks (Sec.2). At that,
 298 the sw-emission may be effectively absorbed by the SR producing the lw-emission, which may in-
 299 crease additionally the band-to-band optical losses. As the sw-emission is more pronounced at low
 300 temperatures ($T < 100$ -120 K), this should lead to a greater difference between LEEs of blue and green
 301 LEDs in this temperature range, in accordance with the data shown in Fig.6b. At high temperatures
 302 ($T \sim 250$ -300 K) the sw-emission is suppressed and the difference between LEEs of blue and green
 303 LEDs in this temperature range (less than $\sim 2\%$) may be attributed to a difference in the band-to-band
 304 light absorption in the MQW active region.

305 Figure 5d shows that the RT EQE dependence on the output power plotted in log scale has a
 306 nearly dome-like character with asymmetric low-power and high-power wings. In this case, the pro-
 307 cedure of the LEE extraction from this dependence based on approximation of the high-power wing
 308 with the ABC-model [6] becomes applicable, providing the LEE value of about 66%. The method used
 309 in our study, which implies two ARs to co-exist, gives the value of 68% which is quite close to the
 310 above cruder estimate.



311

312

313 **Figure 6.** Maximum IQE, light extraction efficiency, quality factors corresponding to lower-wavelength
 314 (Q_{lw}) and shorter-wavelength (Q_{sw}) spectral peaks, and specific optical power (see text for more detail)
 315 as a function of temperature (big symbols). Dash-dotted lines and small circles show for comparison
 316 similar data reported earlier for blue LED [5]. Solid and dotted lines in the plots are drawn for eye.

317 4.2. Quality factors and internal quantum efficiency

318 It has been shown in Sec.3.2 that dependence of EQE of the green LED on output optical power
 319 can be interpreted in terms of two co-existing ARs having different quality factors, Q_{sw} and Q_{lw} , the
 320 temperature dependences of which is given in Figure 6b. One can see from the figure that Q -factors of
 321 the green LED are much lower than those reported in [5] for the blue one. This is manifestation of the
 322 so-called “green gap” problem, i.e. remarkable decline of the LED efficiency towards longer emission
 323 wavelength. Two origins of the “green gap” are commonly discussed: quantum-confined Stark effect
 324 leading to spatial separation of electron and hole wave functions inside the InGaN QWs (see, for ex-
 325 ample, [2,3] and references therein) and degradation of materials quality in InGaN alloys with high
 326 indium content [20,21]. Recently, implication of composition fluctuations in InGaN to the LED effi-
 327 ciency reduction in the “green gap” has been also demonstrated [22,23,24].

328 Figure 6b shows that Q -factor corresponding to sw-emission from the green LED is a few times
 329 lower than that corresponding to the lw-emission. Since the Q -factors determine the maximum IQE
 330 values through the relationship $IQE_k = Q_k / (Q_k + 2)$ ($k = sw, lw$), the lower Q_{sw} results immediately in
 331 a lower IQE values of the sw-emission. The temperature dependences of maximum IQEs for sw- and
 332 lw-emission of the green LED are plotted in Figure 6c. One can see from the figure that the efficiency
 333 of the sw-emission declines with temperature much faster than that of the lw-emission, resulting in
 334 suppression of the sw-peak in the emission spectrum at RT. In turn, IQE corresponding to the lw-
 335 emission of the green LED declines faster than the efficiency of blue LED. This observation is in line
 336 with the conclusion made in [23] that contribution of Auger recombination to the temperature-de-
 337 pendent IQE reduction is much stronger in green LEDs than in blue ones.

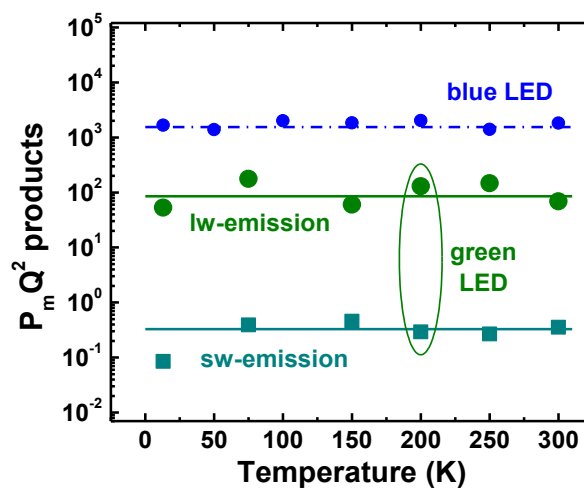
338 Figure 6c shows also that absolute maximum of IQE is controlled by the lw-emission irrespective
 339 of temperature. The maximum IQE tends to the value of $\sim 92\%$ at zero temperature, i. e. the non-radi-
 340 ative recombination does not vanish completely at cryogenic temperatures. This makes doubtful esti-
 341 mations of the RT IQE based on comparison of the LED emission intensities measured at cryogenic
 342 and room temperatures.

343 4.3. Specific powers and recombination volumes

344 Output power corresponding to maximum IQEs of the sw- ($P_m^{(sw)}$) and lw-emission ($P_m^{(lw)}$) of
 345 green LED are plotted in Figure 6d versus temperature along with the transition power P_t . The only
 346 temperature-dependent output power P_m of blue LED from [5] is also shown in the figure by the dash-
 347 dotted line just for comparison. One can see that $P_m^{(lw)}$ and P_m of blue LED are rather close to each other
 348 in the whole temperature range of study. In contrast, $P_m^{(sw)}$ is about two orders of magnitude lower
 349 than $P_m^{(lw)}$ and P_m . The reason for this is discussed below in more detail.

350 The transition power P_t is situated between $P_m^{(sw)}$ and $P_m^{(lw)}$ at $T < 200$ K and approaches $P_m^{(sw)}$ at
 351 RT. The latter corresponds to merging of the sw- and lw-emission peaks at $T = 300$ K, as it can be seen
 352 from Figure 2c.

353 In order to get more information from the data obtained, we have plotted in Figure 7 the $P_m Q^2$
 354 products corresponding to sw- and lw-emission peaks *vs.* temperature. Since $P_m Q^2 \propto E_{ph} V_r B^3 / C^2$
 355 where E_{ph} is the energy of emitted photon, V_r is the recombination volume, and B and C are the radi-
 356 ative and Auger recombination coefficients, respectively (see, for example, [18]), the $P_m Q^2$ product
 357 does not include the Shockley-Read-Hall coefficient A responsible for carrier recombination at point
 358 and extended defects. As one can see from Figure 7, the $P_m Q^2$ products of both sw- and lw-emission
 359 peaks are found to be nearly independent of temperature, similar to the case of blue LED [5]. This is
 360 evidence for the fact that both radiative and Auger recombination coefficients in the green LED, like
 361 in the blue one, have qualitatively similar temperature dependence: either ascending or descending.
 362 This result is in qualitative agreement with the recently observed anomalous (ascending) temperature
 363 variation of the radiative recombination coefficient [23], which was attributed to strong hole localiza-
 364 tion by composition fluctuations in InGaN alloys. At that, the Auger recombination coefficients were
 365 found in [23] to increase with temperature in both blue and green LEDs.



366

367 **Figure 7.** $P_m Q^2$ product as a function of temperature plotted for sw- and lw-emission of green LEDs.

368 Big symbols are experimental points, solid lines are drawn for eyes. Data for blue LED reported in [5]

369 are also shown for comparison by small circles and dash-dotted line.

370 Using the values of the B - and C -coefficients at 450 and 540 nm reported in [25] for RT, we have
 371 estimated the ratio of the recombination volumes of blue LED ($V_r^{(b)}$) and that corresponding to lw-
 372 emission of green LED ($V_r^{(lw)}$). The obtained ratio $V_r^{(b)} / V_r^{(lw)} \approx 0.85$ indicates that the recombination
 373 volumes are comparable with each other. As the active region of the blue LED was specially optimized
 374 to provide a uniform carrier injection in all five QWs in the active region, the latter fact enables attrib-
 375 uting the lw-emission of green LED to operation of its active region as a whole.

376 A similar estimation provides $V_r^{(b)} / V_r^{(sw)} \approx 220$, which demonstrates the recombination volume
 377 of the SR responsible for sw-emission to be about two orders of magnitude smaller than that of the SR
 378 producing lw-emission. Such a big difference cannot be explained by dominant carrier injection in one
 379 of the five QWs. Therefore, a natural interpretation of the result implies the sw-emission comes from
 380 the local lateral areas distributed within the QWs.

381 4.4. Possible origins of active region non-uniformity

382 Any interpretation of the above results should account for and/or explain four main points: (i)
 383 the difference between the wavelengths of sw- and lw-emission, (ii) the sequence of sw- and lw-peaks
 384 appearance in the emission spectrum with the operating current, (iii) the difference in the recombina-
 385 tion volumes associated with sw- and lw-emission, and (iv) the difference in the Q -factors or IQEs of
 386 the sw- and lw-emission. We will consider below a number of scenarios for the active region non-
 387 uniformity, addressing these points.

388 The difference in the emission wavelength can be attributed to variation of either composition or
 389 width of InGaN QWs in the LED active region. Simulations of InGaN SQW LED structures operating
 390 at the current density of 20 A/cm² carried out with the commercial SiLENSe 5.10 package [26] have
 391 shown that the observed difference between the sw- and lw-emission wavelengths may be associated
 392 with either ~2% variation of the indium content in the InGaN alloy or ~0.4 nm (i. e. ~1.5 monolayer)
 393 variation of the QW width. Both versions seem to be realistic for green LEDs examined here.

394 A possible mechanism producing compositional non-uniformity of the active region is partial
 395 stress relaxation in the LED structure. Indeed, the critical thickness of (0001) InGaN/GaN layer is com-
 396 parable with the QW widths in the green spectral range [27]. If the total width of all QWs in the LED
 397 active region exceeds the critical thickness, stress relaxation becomes possible, resulting, in particular,
 398 in an increase of indium content just by a few percent in the top partially relaxed QWs [28]. The ap-
 399 pearance of the sw-emission at low currents and of lw-emission at high currents may be then ex-
 400 plained, assuming dominant hole injection into the bottom (unrelaxed) QWs at low currents. This as-
 401 sumption does not agree, however, with the data of experiments carried out on LEDs with color-coded
 402 blue/cyan QWs in the active region [29]. In addition, the above scenario cannot explain a lower IQE of
 403 the sw-emission, as compared to lw-emission, and the substantial difference in their recombination
 404 volumes.

405 A similar conclusion can be made about another mechanism, which implies the lw-emission to
 406 come from the In-rich clusters more or less uniformly distributed over all the QWs. Here lw-emission
 407 is expected to appear first at low currents and its recombination volume should be smaller than that
 408 of the sw-emission, in contrary to observations. Two-peak emission spectra may also be explained by
 409 contribution of excited states of electrons and holes in InGaN QWs. However, the expected sequence
 410 of lw- and sw-peak appearance in the spectra under increase of operating current (lw-peak at low
 411 currents and sw-peak at high currents) contradicts to our observations as well. Therefore, other mech-
 412 anisms are necessary to invoke in order to interpret the characterization data of our green LEDs.

413 Here, we suggest the following qualitative model for the active region non-uniformity. First of
 414 all, we assume rarely distributed regions with lower indium content responsible for sw-emission to
 415 be embedded into the matrix of InGaN with higher indium content, which is responsible for lw-emis-
 416 sion. These low-indium regions have a lower height of the potential barriers formed at the InGaN/GaN
 417 interfaces for both electrons and holes. This is due to lower band offsets in both conduction and va-
 418 lence bands and lower polarization charges induced at the interfaces. At low LED operating currents,
 419 the carrier injection into the InGaN QWs is limited by thermionic emission over the barriers. Therefore

420 pinching of the current is expected to occur in such a way, as to produce dominant pumping of the
 421 low-indium regions and, eventually, the sw-emission of photons. At higher currents, pumping of the
 422 high-indium matrix starts to occur, resulting in the lw-emission, which becomes quickly dominant
 423 partly due to a much larger recombination volume.

424 Such a scenario is consistent with most of observations discussed above but it does not yet explain
 425 the difference in IQEs (Q -factors) of the sw- and lw-emission regions. The explanation can be given,
 426 assuming the low-indium regions to be formed around extended defects like threading dislocations
 427 and V-pits. Indeed, less effective indium incorporation is expected next to the dislocation cores be-
 428 cause of excess elastic energy related to dislocation-mediated strain. Formation of the InGaN QWs
 429 with larger bandgap on the side walls of V-pits has been directly demonstrated in [30]. Existence of
 430 dislocation cores serving as non-radiative recombination centers may explain a lower IQE of the sw-
 431 emission regions.

432 In order to assess whether the small recombination volume $V_r^{(sw)}$ may be attributed to extended
 433 defects, we assume the sw-emission to originate from the carriers collected from the area of about
 434 $L_d^2 = D_a \tau_d$ around each of the defects, where L_d is the carrier diffusion length, D_a is the ambipolar
 435 diffusion coefficient, and τ_d is the differential carrier life time. Using experimental values $D_a \sim 0.25$
 436 cm^2/s [31] and $\tau_d \sim 20$ ns [23] typical for green InGaN LEDs operating at low currents, we obtain L_d^2
 437 $\sim 5 \times 10^{-9}$ cm^2 . In this case, the density of the extended defects necessary to provide the ratio
 438 $V_r^{(b)} / V_r^{(sw)} \sim 220$ is $\sim 10^6$ cm^{-2} , which may be tentatively associated with the density of V-pits. Indeed,
 439 the carrier injection into semi-polar QWs formed at the side walls of V-pits is not hindered by high
 440 potential barriers typically induced at the {0001}-interfaces of polar QWs. Therefore, the current flow
 441 through the V-pits may dominate under low-current conditions [32]. This conclusion is indirectly sup-
 442 ported by the experimental correlation between the waving observed in I-V curves, which is the evi-
 443 dence for carrier leakage through extended defects, and the values of the current corresponding to
 444 maxima of the sw-emission efficiency (closed circles in Fig.1). Of course, the V-pit density of $\sim 10^6$ cm^{-2}
 445 is just the lower-limit estimate, which does not account for the complex mechanism of current pinch-
 446 ing around this type of defect [32] and dispersion of their dimensions affecting the current flow as
 447 well.

448 It is interesting that two-peak character of the low-temperature efficiency dependence on current
 449 has been reported earlier for both blue and green LEDs [7]. Moreover, the efficiency maxima were
 450 shifted remarkably to lower currents in green LEDs compared to blue ones, in line with our observa-
 451 tions. Those data may also be interpreted in terms of competition between the current flow through
 452 the V-pits and through the {0001}-interfaces of QWs, assuming the efficiency of the main QWs to be
 453 somewhat lower than that of the semi-polar QWs on the side walls of the pits. At RT, the low-current
 454 efficiency peaks quenched and the efficiency dependence on current gains conventional dome-like
 455 shape [7].

456 Generally, the above mechanism considering V-pits as the origin of AR non-uniformity is ex-
 457 pected to be especially pronounced in green LEDs, as higher indium content in the QWs is known to
 458 favor the V-pit formation.

459 5. Conclusions

460 In this study, we have observed mutually correlated non-ordinary evolution of the LED emission
 461 spectra and efficiency which, to our best knowledge, had not been reported before. The observation
 462 could be interpreted in terms of the active region non-uniformity, assuming co-existence of, at least,
 463 two sub-regions emitting at different wavelengths and having different radiative efficiencies. The use
 464 of the ABC-model extended to the case of non-uniform active region enabled estimating the recombi-
 465 nation volumes corresponding to these sub-regions, which were found to differ by a factor of ~ 220 . To
 466 explain such a big difference, as well as the sequence of appearance of the sw- and lw-emission in the
 467 integral spectra, one of the sub-regions was associated with extended defects, like V-pits, whereas
 468 another sub-region was attributed to the main part of the LED active region. As higher indium content

469 in InGaN QWs favors the V-pit formation during LED structure growth, the above observations
470 should be regarded as those specific for green LEDs and much less typical for blue ones.

471 Characterization of the green LED in a wide temperature range from 13 K to 300 K allowed eval-
472 uating temperature-dependent LEE and IQE. The estimated efficiency of light extraction, 68% at RT,
473 was slightly lower than that reported earlier for blue LEDs but it tended to saturate at low tempera-
474 tures at the value of 72%, which was tentatively related to re-absorption of the sw-emission by the lw-
475 emission sub-region. Maximum IQE of the green LED was found to decrease from ~91% at 13 K to
476 ~70% at 300 K and controlled by the lw-emission from the main part of the active region. Remarkable
477 deviation of the IQE maximum from 100% at cryogenic temperatures indicates that non-radiative re-
478 combination does not vanish in the green LED, in contrast to blue one where it was ~97% [5]. This
479 makes doubtful the method of IQE determination based on comparison of EL intensity at cryogenic
480 and room temperatures.

481 Defect-mediated sw-emission approaches its maximum efficiency at very low currents, produc-
482 ing additional peak/shoulder in the EQE dependence on current. It looks like in the previous studies,
483 IQE of the defect-mediated emission exceeded that of the main active region. This resulted in a strong
484 shift of the total IQE/EQE maximum of green LEDs to lower currents, as compared to the case of blue
485 LEDs. In our study, the lw-emission from the main active region dominated at all temperatures. There-
486 fore, the IQE/EQE maximum of the green LED is approached at nearly the same currents as in the case
487 of blue LED examined in [5].

488 Processing of the characterization data has shown that the B^3 / C^2 ratio, where B is the radiative
489 and C is the Auger recombination coefficients, is nearly independent of temperature in both cases of
490 sw- and lw-emission of green and blue LEDs. Accounting for rather strong temperature dependence
491 of single B and C coefficients reported in [23], this fact implies existence of a universal relationship
492 between the recombination coefficients in InGaN QWs irrespective of their particular composition.
493 The physics behind this observation is one of the still open questions to be addressed by future studies.

494 **Acknowledgments:** This work was supported by European Union FP7, NEWLED project, Grant number 318388.
495 The authors greatly appreciate Osram Opto Semiconductors for providing LED samples and Dr. Benjamin
496 Haskell for thoughtful comments.

497 **Author Contributions:** I.E. Titkov designed, performed the experiments and contributed to the manuscript prep-
498 aration; S.Yu. Karpov developed the paper concept, analytical model and largely contributed to the manuscript
499 preparation; D. Mamedov contributed to the spectral data evaluation; A. Yadav and V.L. Zerova contributed to
500 the experiment, scientific discussion and manuscript preparation; E. Rafailov supervised the project.

501 **Conflicts of Interest:** "The authors declare no conflict of interest."

502

503 **Abbreviations**

504 The following abbreviations are used in this manuscript:

505	AR	Active region
506	EQE	External quantum efficiency
507	EL	Electroluminescence
508	IQE	Internal quantum efficiency
509	LED	Light-emitting diode
510	LEE	Light extraction efficiency
511	LO	Longitudinal optical
512	MQW	Multiple quantum well
513	ND	Neutral density
514	QW	Quantum well
515	RT	Room temperature
516	SQW	Single quantum well
517	WPE	Wall plug efficiency

518 **References**

-
- [1] Zheludev, N. The life and times of the LED a 100-year history. *Nat. Photonics* **2007**, *1*, 189-129, doi:10.1038/nphoton.2007.34.
- [2] Crawford, M. H. LEDs for Solid-State Lighting: Performance Challenges and Recent Advances. *IEEE J. Sel. Top. Quantum Electron.*; **2009**, *15*, 1028-1040, doi: 10.1109/JSTQE.2009.2013476.
- [3] Weisbuch, C.; Piccardo, M.; Martinelli, L.; Iveland, J.; Peretti, J.; and Speck, J.S. The efficiency challenge of nitride light-emitting diodes for lighting. *Phys. Status Solidi A* **2015**, *212*, 899-913, doi:10.1002/pssa.201431868.
- [4] Broell, M.; Sundgren, P.; Rudolph, A.; Schmidt, W.; Vogl, A. and Behringer, M. New developments on high efficiency infrared and InGaAlP light emitting diodes at OSRAM Opto-Semiconductors. *Proc. SPIE* **2014**, 90030L, doi: 10.1117/12.2039078.
- [5] Titkov, I.E.; Karpov, S.Yu.; Yadav, A.; Zerova, V.L.; Zulonias, M.; Galler, B.; Strassburg, M.; Pietzonka, I.; Lugauer, H.-J.; and Rafailov, E.U. Temperature-Dependent Internal Quantum Efficiency of Blue High-Brightness Light-Emitting Diodes. *IEEE J. Quantum Electron.* **2014**, *50*, 189-129, doi: 10.1109/JQE.2014.2359958.
- [6] Karpov, S.Yu.; Binder, M.; Galler, B.; and Schiavon, D. Spectral dependence of light extraction efficiency of high-power III-nitride light-emitting diodes. *Phys. Status Solidi RRL* **2015**, *1*, 189-129, doi: 10.1002/pssr.201510073.
- [7] Peter, M.; Laubsch, A.; Bergbauer, W.; Meyer, T.; Sabathil, M.; Baur, J.; and Hahn, B. New developments in green LEDs. *Phys. Status Solidi A* **2007**, *1*, 189-129, doi: 10.1002/pssa.200880926.
- [8] Shin, D.-S.; Han D.-P.; Oh, J.-Y and Shim, J.-I Study of droop phenomena in InGaN-based blue and green light-emitting diodes by temperature-dependent electroluminescence. *Appl. Phys. Lett.* **2012**, *100*, 153506, doi: 10.1063/1.3703313.
- [9] Dai, Q.; Shan, Q.; Cho, J.; Schubert, E.F.; Crawford, M.H.; Koleske, D.D.; Kim, M.-H; and Park, Y. On the symmetry of efficiency-versus-carrier-concentration curves in GaInN/GaN light-emitting diodes and relation to droop-causing mechanisms. *Appl. Phys. Lett.* **2011**, *98*, 033506, doi: 10.1063/1.3544584.
- [10] Lin, G.-B.; Meyaard, D.; Cho, J.; Schubert, E.F.; Shim, H. and Sone, C. Analytic model for the efficiency droop in semiconductors with asymmetric carrier-transport properties based on drift-induced reduction of injection efficiency. *Appl. Phys. Lett.* **2012**, *100*, 161106, doi: 10.1063/1.4704366.
- [11] Wang, J.; Wang, L.; Wang, L.; Hao, Z.; Luo, Y.; Dempewolf, A.; Müller, M.; Bertram, F.; and Christen, J. An improved carrier rate model to evaluate internal quantum efficiency and analyze efficiency droop origin of InGaN based light-emitting diodes. *Appl. Phys. Lett.* **2012**, *102*, 023107, doi: 10.1063/1.4736591.
- [12] Kisin, M.V. and El-Ghoroury, H.S. Inhomogeneous injection in III-nitride light emitters with deep multiple quantum wells. *J. Comput. Electron.* **2015**, *14*, 432-443, doi: 10.1007/s10825-015-0673-5.
- [13] Karpov, S.Yu. Effect of localized states on internal quantum efficiency of III-nitride LEDs. *Phys. Status Solidi RRL* **2010**, *4*, 320-322, doi: 10.1002/pssr.201004325.
- [14] Laubsch, A.; Sabathil, M.; Baur, J.; Peter, M. and Hahn, B. High-Power and High-Efficiency InGaN-Based Light Emitters. *IEEE Trans. Electron. Devices* **2010**, *57*, 79-87, doi: 10.1109/TED.2009.2035538.

-
- [15] Shah, J. M.; Li, Y.-L.; Gessmann, Th. and Schubert, E.F. Experimental analysis and theoretical model for anomalously high ideality factors ($n_{2,0}$) in Al-GaN/GaN p-n junction diodes. *J. Appl. Phys.* **2003**, *94*, 2627-2630, doi: 10.1063/1.1593218.
- [16] Masui, H. Diode ideality factor in modern light-emitting diodes. *Semicond. Sci. Technol.* **2011**, *26*, 075011, doi: 10.1088/0268-1242/26/7/075011.
- [17] Cao, X. A.; LeBoeuf, S. F.; Rowland, L. B. and Liu, H. Temperature-Dependent Electroluminescence in InGaN/GaN Multiple-Quantum-Well Light-Emitting Diodes. *J. Electronic Materials* **2003**, *32*, 316-321, doi: 10.1007/s11664-003-0151-x
- [18] Karpov, S. Yu. ABC-model for interpretation of internal quantum efficiency and its droop in III-nitride LEDs: a review. *Opt. Quant. Electron.* **2015**, *47*, 1293-1303, doi:10.1007/s11082-014-0042-9.
- [19] Karpov, S.Yu.; Cherkashin, N.A.; Lundin, W.V.; Nikolaev, A.E.; Sakharov, A.V.; Sinitsyn, M.A.; Usov, S.O.; Zavarin, E.E. and Tsatsulnikov, A.F. Multi-color monolithic III-nitride light-emitting diodes: Factors controlling emission spectra and efficiency. *Phys. Status Solidi A* **2016**, *213*, 19-29, doi: 10.1002/pssa.201532491.
- [20] Langer, T.; Jönen, H.; Kruse, A.; Bremers, H.; Rossow, U. and Hangleiter, A. Strain-induced defects as non-radiative recombination centers in green-emitting GaInN/GaN quantum well structures. *Appl. Phys. Lett.* **2013**, *103*, 022108, doi: 10.1063/1.4813446.
- [21] Hammersley, S.; Kappers, M.J.; Massabuau, F.C.-P.; Sahonta, S.-L.; Dawson, P.; Oliver, R. A. and Humphreys, C. J. Effects of quantum well growth temperature on the recombination efficiency of InGaN/GaN multiple quantum wells that emit in the green and blue spectral regions. *Appl. Phys. Lett.* **2015**, *107*, 132106, doi: 10.1063/1.4932200.
- [22] Auf der Maur, M.; Pecchia, A.; Penazzi, G.; Rodrigues, W. and Di Carlo, A. Efficiency Drop in Green InGaN/GaN Light Emitting Diodes: The Role of Random Alloy Fluctuations. *Phys. Rev. Lett.* **2016**, *116*, 027401, doi: 10.1103/PhysRevLett.116.027401.
- [23] Nippert, F.; Karpov, S. Yu.; Callsen, G.; Galler, B.; Kure, T.; Nenstiel, C.; Wagner, M. R.; Straßburg, M.; Lugauer, H.-J. and Hoffmann, A. Temperature-dependent recombination coefficients in InGaN light-emitting diodes: Hole localization, Auger processes, and the green gap. *Appl. Phys. Lett.* **2016**, *109*, 61103, doi: 10.1063/1.4965298.
- [24] Karpov, S.Yu. Carrier localization in InGaN by composition fluctuations: implication to “green gap”. *Photon. Res.* **2017**, *5*, A7-A12, doi: 10.1364/PRJ.5.0000A7.
- [25] Schiavon, D.; Binder, M.; Peter, M.; Galler, B.; Drechsel, P. and Scholz, F. Wave-length-dependent determination of the recombination rate coefficients in single-quantum-well GaInN/GaN light emitting diodes. *Phys. Status Solidi B* **2013**, *250*, 283-290, doi: 10.1002/pssb.201248286.
- [26] SiLENSe—software tool for light emitting diode (LED) bandgap engineering. Available online: <http://www.str-soft.com/products/SiLENSe/index.htm> (accessed on 03 July 2017).
- [27] Lobanova, A. V.; Kolesnikova, A. L.; Romanov, A. E.; Karpov, S. Yu.; Rudinsky, M. E. and Yakovlev, E. V. Mechanism of stress relaxation in (0001)InGaN/GaN via formation of V-shaped dislocation half-loops. *Appl. Phys. Lett.* **2013**, *103*, 152106, doi: 10.1063/1.4824835.
- [28] Sakharov, A.V.; Lundin, W.V.; Zavarin, E.E.; Sinitsyn, M.A.; Nikolaev, A.E.; Usov, S.O.; Sizov, V.S.; Mikhailovsky, G.A.; Cherkashin, N.A.; Hytch, M.; Hue, F.; Yakovlev, E.V.; Lobanova, A.V. and Tsatsulnikov, A.F. Effect of strain relaxation on formation of active region of InGaN/(Al)GaN heterostructures for green range LEDs. *Semiconductors* **2009**, *43*, 812-817, doi: 10.1134/S1063782609060232.
- [29] Galler, B.; Laubsch, A.; Wojcik, A.; Lugauer, H.; Gomez-Iglesias, A.; Sabathil, M. and Hahn, B. Investigation of the carrier distribution in InGaN-based multi-quantum-well structures. *Phys. Stat. Solidi C* **2011**, *8*, 2372-2374, doi: 10.1002/pssc.201001075.
- [30] Hangleiter, A.; Hitzel, F.; Netzel, C.; Fuhrmann, D.; Rossow, U.; Ade, G. and Hinze, P. Suppression of Non-radiative Recombination by V-Shaped Pits in GaInN/GaN Quantum Wells Produces a Large Increase in the Light Emission Efficiency. *Phys. Rev. Lett.* **2005**, *95*, 127402, doi: 10.1103/PhysRevLett.95.127402.
- [31] Danhof, J.; Solowan, H.-M.; Schwarz, U. T.; Kaneta, A.; Kawakami, Y.; Schiavon, D.; Meyer, T. and Peter, M. Lateral charge carrier diffusion in InGaN quantum wells. *Phys. Stat. Solidi B* **2012**, *249*, 480-484, doi: 10.1002/pssb.201100476.
- [32] Li, C.-K.; Wu, C.-K.; Hsu, Ch.-Ch.; Lu, L.-Sh.; Li, H.; Lu, T.-Ch. and Wu, Y.-R. 3D numerical modeling of the carrier transport and radiative efficiency for InGaN/GaN light emitting diodes with V-shaped pits. *AIP Advances* **2016**, *6*, 055208. doi: 10.1063/1.4950771.



© 2017 by the authors. Submitted for possible open access publication under the terms and conditions of the Creative Commons Attribution (CC BY) license (<http://creativecommons.org/licenses/by/4.0/>).